International Immunopharmacology 76 (2019) 105864

Contents lists available at ScienceDirect

International Immunopharmacology

journal homepage: www.elsevier.com/locate/intimp

Combined MEK inhibition and tumor-associated macrophages depletion suppresses tumor growth in a triple-negative breast cancer mouse model

Qiulei Zhang[1], Kehao Le[1], Ming Xu, Jun Zhou, Yunxiao Xiao, Wen Yang, Yujia Jiang, Zihan Xi, Tao Huang*

Department of Breast and Thyroid Surgery, Union Hospital, Tongji Medical College, Huazhong University of Science and Technology, 430022 Wuhan, China

ARTICLE INFO

Keywords:
Triple-negative breast cancer
Tumor-associated macrophages
MAPK pathway
Proliferation
4 T1 cells

ABSTRACT

Tumor-associated macrophages (TAMs) are closely related to poor prognosis in triple-negative breast cancer (TNBC). Thus, gaining insight into how TAMs support cancer progression could contribute to effective therapies. We utilized the 4 T1 murine TNBC cell line and murine bone marrow-derived macrophages to assess TAM-mediated pro-proliferative effects in vivo and in vitro. Further, Transcriptional analysis was performed to identify pathways activated in TAM-stimulated 4 T1 cells. We also explored the therapeutic efficacy of combining a mitogen-activated protein kinase kinase (MEK) inhibitor with TAM-targeted therapy using a TNBC mouse model. We found that the presence of TAMs was significantly associated with proliferating cancer cells in a TNBC mouse model. Moreover, RNA sequencing analysis showed that TAMs could enhance mitogen-activated protein kinase (MAPK) pathway activation in 4 T1 cells compared to that in control cells. Further, the depletion of TAMs by clodronate liposomes significantly reduced MAPK pathway activation in vivo. In addition, the blockade of MAPK signaling by a MEK inhibitor repressed TAM-mediated cancer cell proliferation. Most importantly, MEK inhibition combined with macrophage depletion significantly suppressed tumor growth and increased T lymphocyte infiltration in a TNBC model. Our study suggests the possibility that TAM-induced MAPK pathway activation promotes cancer cell proliferation. Thus, MEK inhibition combined with macrophage depletion might represent an effective treatment for TNBC.

1. Introduction

In China, breast cancer is the leading cause of cancer-related death in women younger than 45 years and it is projected to account for 15% of all newly-diagnosed cancers in females [1]. Triple-negative breast cancer (TNBC) is a heterogeneous subtype characterized by high proliferation, high histological grade, and features associated with poor prognosis due to limited effective treatment options [2]. Despite the fact that TNBC patients have higher response rates to neoadjuvant chemotherapy, recurrence is more commonly observed in this type of breast cancer [3]. Therefore, effective therapeutic targets to treat this disease subtype are urgently needed.

Tumor-associated macrophages (TAMs), the most abundant leukocytes in the tumor microenvironment, support the tumor by promoting angiogenesis, secreting growth factors, and suppressing adaptive immunity [4,5]. Clinical evidence has shown that increased TAMs positively correlate with poor prognosis in breast cancer patients [6–8]. Accordingly, the depletion of TAMs has been reported to reduce tumor growth in breast cancer mouse models [9,10]. In addition, previous studies have shown that TNBC cell lines have the strongest ability to activate macrophages to induce a TAM-like phenotype [11,12], indicating that interactions between TNBC cells and TAMs can contribute to cancer progression. Thus, TAMs could be an interesting therapeutic target for patients with TNBC.

The mitogen-activated protein kinase (MAPK) pathway is one of the best-characterized kinase cascades in cancer cell biology. Aberrant activation of this pathway by growth factors or activating mutations in oncogenic kinases can lead to the continuous stimulation of cell growth [13,14]. The combination of single-cell RNA and protein analytical platforms has revealed that stromal cells contribute to the proliferative phenotype of pancreatic cancer through the MAPK pathway [15]. MAPK pathway activation is also one of the most important intrinsic properties of TNBC [16]. However, studies have not elucidated the relationship between TAMs and this pathway in TNBC, in addition to

* Corresponding author at: Department of Breast and Thyroid Surgery, Union Hospital, Tongji Medical College, Huazhong University of Science and, Technology, 1277 Jiefang Avenue, Wuhan 430022, Hubei, China.
E-mail address: huangtaowh@163.com (T. Huang).
[1] Qiulei Zhang and Kehao Le contributed equally to this work.

https://doi.org/10.1016/j.intimp.2019.105864
Received 12 July 2019; Received in revised form 22 August 2019; Accepted 23 August 2019
Available online 31 August 2019

whether TAMs contribute to tumor growth through MAPK pathway activation.

In this study, a TNBC mouse model was used to study the supporting effects of TAMs in vivo, and a co-culture system of TAMs and 4 T1 cells was established in vitro to explore the mechanism underlying the pro-proliferative effect of TAMs. We also explored the therapeutic efficacy of TAM-depletion in combination with a MAPK signaling inhibitor for the treatment of TNBC.

2. Materials and methods

2.1. Cell line and mice

Murine 4T1breast cancer cells were purchased from the American Type Culture Collection (Manassas, VA, USA), and were maintained in MEM supplemented with 10% fetal bovine serum (FBS). The human MDA-MB-231 TNBC cell line was purchased from the Cell Bank of the Chinese Academy of Sciences (Shanghai, China). These cells were cultured in Leibovitz's 15 medium supplemented with 10% FBS. Both lines were incubated in humidified 37 °C conditions. Female BALB/c mice, 8–10 weeks, were purchased from the Experimental Animal Center of Wuhan University and were housed in a specific pathogen-free facility at the Experimental Animal Center (Tongji Medical College of Huazhong University of Science and Technology, Wuhan, China). The care of and experimentation with mice were performed in accordance with institutional guidelines under protocols approved by the Institutional Animal Care and Use Committee at the animal care unit of Huazhong University of Science and Technology, Wuhan, China.

2.2. M2 polarized bone marrow-derived macrophages and conditioned media

Mouse bone marrow cells were harvested from femurs of female BALB/c mice, and then re-suspended in complete DMEM medium with 50 ng/mL murine M-CSF (Peprotech, USA) in a 100-mm Petri dish. After 4 days, half the medium was replaced with complete DMEM medium with 25 ng/mL murine IL-4 (Peprotech, USA) to induce differentiation into the M2 phenotype. Macrophage purity was determined by flow cytometry. Conditioned medium was prepared from M2 polarized macrophages cultured for 24 h at a seeding concentration of 1×10^6/mL.

2.3. 4 T1 cell co-culture with M2 macrophages

4 T1 cells (1×10^5) were plated in 6-well plates with 2 mL medium. After 12 h, M2 macrophages (5×10^5) were plated onto 0.4-mm pore inserts in the upper chambers of 6-well transwell plates with 1.5 mL medium. Co-culture systems were maintained for an additional 72 h.

2.4. Evaluation of proliferation

The Cell Counting Kit-8 (CCK-8) (BOSTER, China) was used to evaluate cell proliferation following the manufacturer's instructions.

2.5. 4 T1 mouse model of breast cancer

4 T1 tumor cells (5×10^5) were injected, either alone or mixed with M2-macrophages (1×10^5), into the mammary fat pads of BALB/c mice. Selumetinib (Target Molecule Corp, USA), a highly potent MEK inhibitor, was intraperitoneally injected at 50 mg/kg once daily. The volume of the tumor was calculated as follows: volume = (length × width × width)/2.

2.6. Macrophage depletion

We used clodronate liposomes (From Vrije Universiteit, Amsterdam) to deplete macrophages in vivo. A dose of 100 μL of clodronate liposomes was orthotopically injected into the mammary fat pads of BALB/c mice, and 24 h later, 4 T1 cells (5×10^5) mixed with 100 μL PBS or clodronate liposomes were injected into the same fat pads. Next, clodronate lipsomes were injected around the tumor implantation sites once every other day for 4 weeks.

2.7. Quantitative real-time PCR and western blotting

Total RNA was extracted using TRIzol reagent (Takara, Shiga, Japan). The RNA samples were reverse transcribed into cDNA using the ReverTra Ace qPCR RT Kit (Toyobo, Osaka, Japan). The levels of target gene mRNA transcripts relative to the control β-actin were determined by quantitative RT-PCR analyses on a Roche Light Cycler 480 System using SYBR Green Real Time PCR Master Mix (Toyobo) and specific primers. The data were normalized to β-actin levels and analyzed by the $2^{-\Delta\Delta Ct}$ method. The sequences of primers are shown in Supplementary Table 1.

The procedure for western blotting was described in our previous study [17]; briefly, 4 T1 cells were washed twice with ice-cold PBS and lysed in RIPA buffer and boiled with 5× loading buffer. After electrophoresis and membrane transfer, the target proteins were probed with the following primary antibodies: anti-GAPDH (1:1000, Proteintech Group, China), anti-Phospho-Erk1/2(Thr202/Tyr204) (1:2000, Cell Signaling Technology, USA), and anti-Erk1/2(1:1000, Cell Signaling Technology, USA).

2.8. Immunofluorescence

The biopsied mouse breast tumor sections (4-μm) were stained with rabbit anti-p-ERK1/2 (1:200, Cell Signaling Technology, USA) or rabbit anti-Ki67 (1:200, Abcam, UK) and goat anti-mouse CD206 (1:200, RD, USA) overnight at 4 °C. The bound antibodies were detected with FITC-donkey anti-goat antibody and PE-donkey anti-rabbit antibody (1:400, Jackson ImmunoResearch, USA) and nuclei were stained with DAPI (Sigma, USA). The cells were analyzed by laser confocal microscopy (Olympus, Japan).

2.9. RNA-sequencing

Total RNA was extracted from the control macrophages and those co-cultured with 4 T1 cells using TRIzol® Reagent according the manufacturer's instructions (Invitrogen, USA) and genomic DNA was removed using DNase I (TaKara, Japan). Subsequent sequencing was conducted by Majorbio (Shanghai, China).

2.10. Flow cytometry

Mouse tumors were minced and digested with 1 mg/mL collagenase D at 37 °C for 2 h. After erythrocyte lysis, the cells were washed with PBS and stained with anti-CD4-FITC, anti-CD8-PE, anti-F4/80-PE, anti-CD11b-APC-CY7, anti-CD206-APC (all BD PharMingen, USA), and isotype IgG for 30 min at 4 °C. The 4 T1 cells in different groups were fixed, permeabilized, and intracellularly stained with rabbit antibody against phospho-Erk1/2 (Thr202/Tyr204; 1:800, Cell Signaling Technology, USA) for 60 min at 4 °C. Next, samples were incubated with FITC-donkey anti-rabbit antibody (1:400, Jackson ImmunoResearch, USA) for 30 min at room temperature. The cells were characterized by flow cytometry (BD LSR Fortessa X-20) and the data were analyzed using FlowJo software.

2.11. Statistical analysis

Colony formation assays and fluorescent signals from immunofluorescence staining were quantified using ImageJ version 1.37 V. Statistical analyses were performed using SPSS version 17.0 and

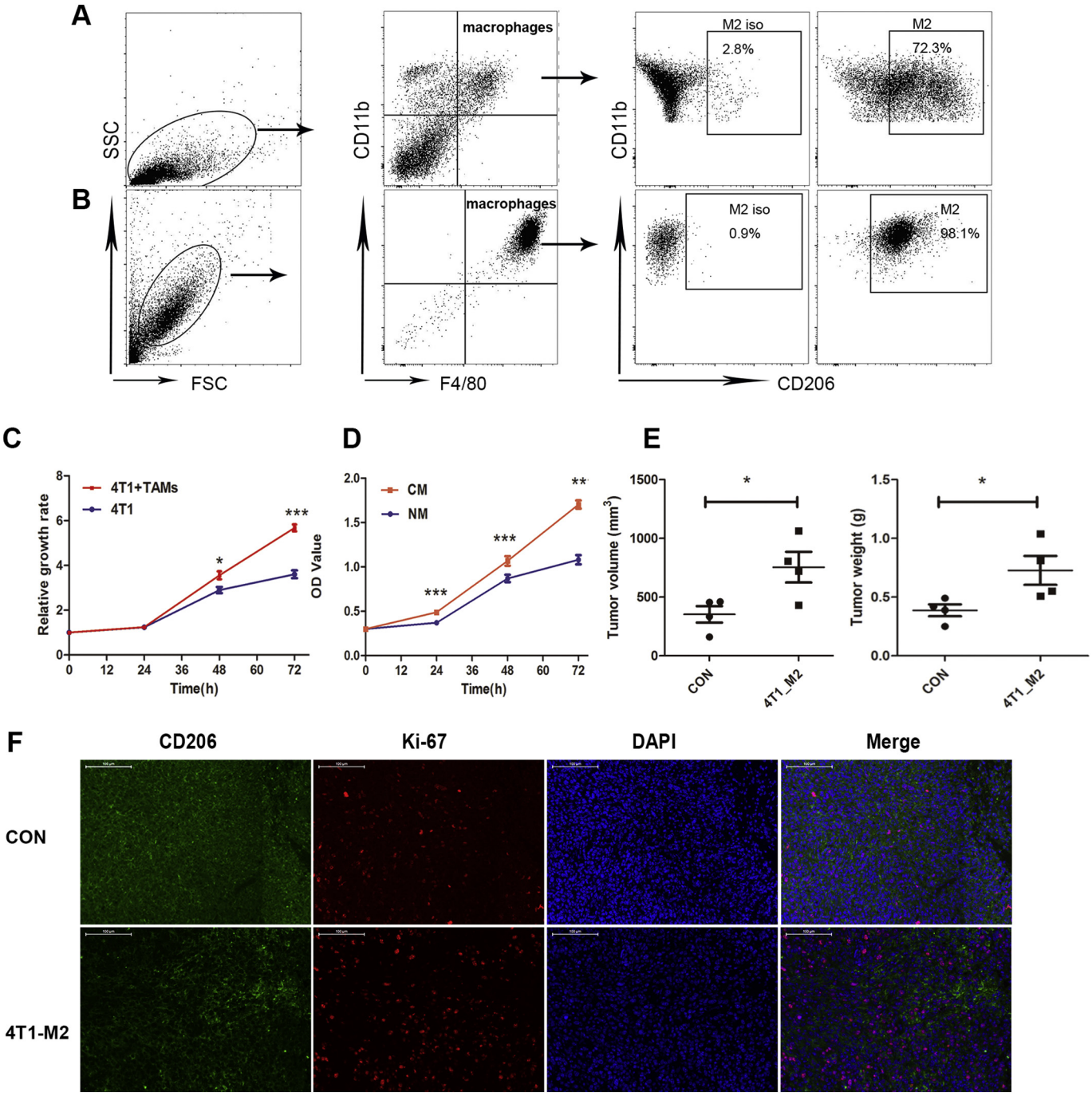

Fig. 1. Tumor-associated macrophages (TAMs) enhance 4 T1 breast cancer growth.
Representative flow cytometric analyses of $CD11b^+$ $F4/80^+$ $CD206^+$ tumor-associated macrophages (TAMs) among monocytes from 4 T1 mammary tumors (A) and the purity of $CD11b^+$ $F4/80^+$ $CD206^+$ M2 macrophages from the bone marrow of mice after M-CSF and IL-4 induction (B) was tested. (C) 4 T1 cells (1×10^3) were cultured alone or co-cultured with 5×10^2 M2 macrophages in 96-well plates for 72 h. The relative growth rate of the control group (blue) and the M2 macrophage co-cultured group (red) ($n = 5$) was assessed by CCK-8 assays. (D) 4 T1 cells were treated with normal culture medium (blue) or 30% M2 macrophage-conditioned medium (red) for 72 h. Cell proliferation was assessed by CCK-8 assays (n = 5). (E) Tumor volumes (mm^3) and tumor weights (g) in individual groups of mice ($n = 4$). (F) Immunofluorescence staining of CD206 (green) and Ki-67 (red) in the tumor tissues from the control group (upper) and from the group co-injected with M2 macrophages (lower) based on confocal microscopy. Cell nuclei were stained with DAPI (blue). Scale bars = 100 μm. Original magnification, ×200. Data are representative images or expressed as the mean ± SEM of each group from three separate experiments, $^*p < 0.05$, $^{**}p < 0.01$, $^{***}p < 0.001$. (For interpretation of the references to colour in this figure legend, the reader is referred to the web version of this article.)

GraphPad Prism version 5.0. The differences between groups were analyzed using an unpaired Student *t*-test and the differences among the groups were analyzed by one-way analysis of variance (ANOVA). The Kaplan–Meier method was used to estimate survival. Differences were considered significant at $P < 0.05$. The asterisks indicate *P < 0.05, $^{**}P < 0.01$, and $^{***}p < 0.001$. Data are presented as the mean ± SEM.

3. Results

3.1. TAMs enhance TNBC tumor growth

TAMs comprise a diverse collection of cell types with distinct functions in the tumor microenvironment. We performed flow cytometry to analyze the features of TAMs isolated from 4 T1 mammary tumors. Our findings were consistent with previous studies that TAMs in breast cancer are primarily a subpopulation with an M2 phenotype (Fig. 1A) [18,19]. To investigate whether TAMs promote the proliferation of 4 T1 cells in vitro, we isolated monocytes from the bone marrow of BALB/c mice and then treated them with M-CSF and IL-4 to induce the M2 phenotype (Fig. 1B). As shown in Fig. 1C, incubation with M2 macrophages significantly stimulated the proliferation of breast cancer cells compared to that with the vehicle control. We next investigated whether the supernatant from M2 macrophages could exert the same pro-proliferative effect. Similarly, treatment with 30% M2 macrophage-conditioned medium also remarkably promoted cell proliferation (Fig. 1D). For the breast cancer mouse model, 4 T1 cells were injected into the mammary fat pads of BALB/c mice either alone

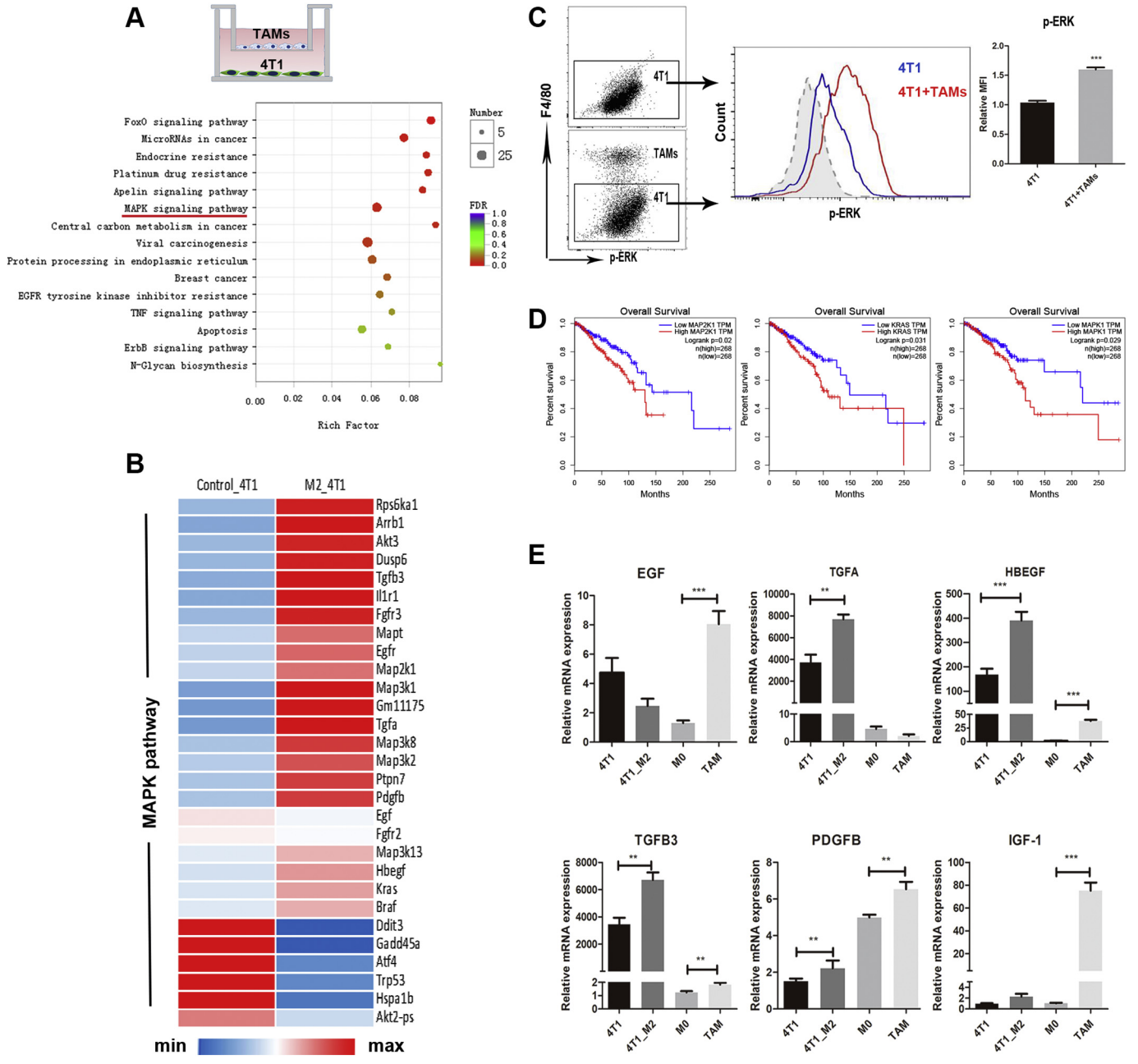

Fig. 2. Tumor-associated macrophages (TAMs) enhance MAPK pathway activation in tumor cells.
(A) KEGG pathway analyses of significantly upregulated pathways in 4 T1 cells after co-culture with TAMs for 72 h. (B) Heatmap showing changes in MAPK pathway-related genes. (C) Representative flow cytometric analyses of phosphorylated ERK1/2 levels in 4 T1 cells (blue) or 4 T1 cells co-cultured with TAMs (red) for 24 h, Iiotype-stained cells are shown in grey. Relative mean fluorescence intensity (MFI) of phosphorylated ERK1/2 in 4 T1 cells is shown in each group at right ($n = 4$). (D) Kaplan–Meier analysis of the association between the expression of MAP2K1, KRAS, and MAPK1 and overall survival in breast cancer patients ($n = 536$). (E) The relative mRNA expression of genes encoding EGF, HB-EGF, IGF-1, TGF-α, PDGFB, and TGFB3 in 4 T1 cells, TAM-treated 4 T1 cells, macrophages, and TAMs was examined by RT-PCR analysis; $n = 6$ in each group. Data are representative images or expressed as the mean ± SEM of each group from three separate experiments, $^{*}p < 0.05$, $^{**}p < 0.01$, $^{***}p < 0.001$. (For interpretation of the references to colour in this figure legend, the reader is referred to the web version of this article.)

or with M2 macrophages. All mice were sacrificed 5 weeks after inoculation. This showed that more TAMs resulted in increased tumor volumes and weights (Fig. 1E). Primary tumor tissue sections from each group were then analyzed by immunofluorescence staining. Interestingly, we found that tumor sections from the co-injection group were highly infiltrated by TAMs ($CD206^+$) and surrounded by proliferating tumor cells ($Ki67^+$) compared to that in the control group (Fig. 1F). These data suggested that TAMs could enhance breast tumor growth.

3.2. TAMs enhance MAPK signaling in 4 T1 cells

We further investigated the underlying mechanisms through which TAMs mediate pro-proliferative effects in 4 T1 cells in vitro. To simulate the tumor microenvironment, M2 macrophages and 4 T1 cells were plated into the upper and lower chambers of transwell co-culture systems, respectively (Fig. 2A). Next, we performed whole transcriptome analysis of 4 T1 cells incubated with vehicle control or M2 macrophages. Kyoto Encyclopedia of Genes and Genomes (KEGG) pathway analyses showed that MAPK signaling was significantly enriched in the M2 macrophages-treated group compared to that in controls (Fig. 2A and B). To further determine whether the MAPK pathway was activated, the phosphorylation of ERK1/2 following M2 macrophage treatment was analyzed by flow cytometry. The results indicated that co-culture with M2 macrophages could significantly enhance the activation of MAPK signaling, as evidenced by increased phosphorylation levels of ERK1/2 (Fig. 2C). Similarly, western blotting showed that treatment with the supernatant from M2 macrophages could increase p-ERK1/2 levels in 4 T1 cells (Supplementary Fig. 1). To clarify the clinical significance of the MAPK pathway in breast cancer, an online Kaplan–Meier analysis tool based on The Cancer Genome Atlas (TCGA) data sets ($n = 536$) revealed that the expression of important genes associated with the MAPK pathway were inversely associated with overall survival in breast cancer (Fig. 2D) [20]. Next, we validated the mRNA expression of genes encoding six growth factors (EGF, HB-EGF, IGF-1, TGF-α, PDGFB, and TGFB3) that can lead to MAPK pathway activation in the TAM–4 T1 co-culture systems. The relative mRNA levels of *EGF*, *IGF-1*, and *PDGFB* were remarkably increased in the 4 T1 cell-treated macrophages. Consistent with RNA sequencing results, TAMs could significantly induce the mRNA expression of *HB-EGF*, *TGFB3*, and *TGF-α* in the 4 T1 cell line (Fig. 2E). Together, these results suggest that TAMs could enhance MAPK signaling in breast cancer cells.

3.3. TAM depletion inhibits TNBC tumor growth and MAPK pathway activation

Our results showed that TAMs significantly induce growth factor expression and MAPK signaling in TNBC cells. Moreover, TAM-mediated transcriptional changes were involved in cancer growth and therapy resistance such as platinum drug, endocrine, and EGFR tyrosine kinase inhibitor resistance (Fig. 2A). These facts might indicate that targeting TAMs is a possible therapeutic strategy for breast cancer. Therefore, we applied clodronate liposomes to selectively deplete tumor-infiltrating macrophages in a 4 T1 breast cancer mouse model. Tumors were surgically removed and weighed on day 35 after clodronate liposome treatment. We found that clodronate liposomes could reduce tumor volumes and weights (Fig. 3A). Further, tumor tissue sections were analyzed by immunofluorescence staining. A significant reduction in TAMs ($CD206^+$) and proliferating tumor cells ($Ki67^+$) were observed in the clodronate liposome-treated group, compared to those in the control group (Fig. 3B). These results indicate that TAMs are significantly associated with proliferating cancer cells in TNBC mouse models. To determine whether MAPK signaling is associated with macrophage infiltration, we evaluated the phosphorylation of ERK1/2 and the quantity of infiltrated TAMs in breast cancer tissues from different groups. Immunofluorescence staining of tumor tissues revealed a significant reduction of p-ERK1/2 levels with decreased $CD206^+$ macrophage infiltration after TAM depletion (Fig. 3C–E). To clarify the relationship between TAMs and MAPK signaling in breast cancer, we evaluated data from the Tumor IMmune Estimation Resource [21]. Correlation analysis from TIMER ($n = 1093$) revealed that MRC1 (CD206) expression was positively associated with MAP2K1 (ERK) in breast cancer (Fig. 3F). These findings suggest that TAM depletion can significantly impair MAPK signaling in a TNBC mouse model.

3.4. Blockade of MAPK signaling represses TNBC cell proliferation

To determine whether blocking MAPK signaling could affect TNBC cell proliferation in vitro, we used selumetinib, a highly potent MEK inhibitor, to block MAPK signaling in 4 T1 cells exposed to the TAM-conditioned medium. 4 T1 cells were treated with increasing amounts selumetinib for 48 h, and cell viability was measured by CCK-8 assays. As shown in Fig. 4A, selumetinib application repressed the proliferation of 4 T1 cells in a dose-dependent manner. The colony formation capacity of 4 T1 cells was also significantly inhibited after drug treatment (Fig. 4B). Similarly, western blot analysis showed that the phosphorylation of ERK1/2 in 4 T1 cells was potently reduced by selumetinib (Fig. 4C). We next investigated whether selumetinib could inhibit TAM-mediated pro-proliferative effects and MAPK signaling in vitro. M2 macrophages were added to the culture dishes with 4 T1 cells, and we found that selumetinib could inhibit 4 T1 cell proliferation based on CCK-8 assays (Fig. 4D). Flow cytometry also indicated that the mean fluorescence intensity (MFI) of p-ERK1/2 in co-cultured 4 T1 cells was significantly reduced by selumetinib treatment compared to that in controls (Fig. 4E). We further examined whether selumetinib could suppress human TNBC cell proliferation in the presence of growth factors. IGF-1and EGF are important growth factors secreted from TAMs [7,22]. First, we applied recombinant human IGF-1 and EGF to MDA-MB-231 cells and observed increased cell proliferation in each group (Fig. 4F). Next, we found that selumetinib could significantly inhibit extracellular growth factor (EGF and IGF-1)-induced proliferation effects based on CCK-8 assays (Fig. 4G). These observations demonstrated that selumetinib could suppress TNBC cell proliferation by blocking MAPK signaling.

3.5. Combining selumetinib with clodronate liposomes suppresses TNBC tumor growth and increases T lymphocyte infiltration

Various preclinical studies have shown that single-agent treatments targeting TAMs have only limited efficacy [23]. Moreover, selumetinib can suppress cancer cell proliferation by blocking MAPK signaling. We thus hypothesized that MEK inhibitors combined with TAM depletion could result in preferable therapeutic effects. To assess this hypothesis, tumor-bearing mice were treated with selumetinib or clodronate liposomes alone or in combination. We found that either alone caused a modest inhibition of tumor growth. However, their combination significantly restrained tumor progression compared to growth in the control group (Fig. 5A). Immunofluorescence staining of tumor tissues revealed high levels of p-ERK1/2 in the control mice tumors, whereas either TAM depletion or selumetinib-treated groups showed markedly reduced levels of p-ERK1/2 expression (Fig. 5B). In addition, flow cytometry demonstrated a decreased frequency of $CD206^+$ TAMs (Fig. 5C and D) and an increased percentage of $CD8^+$ and $CD4^+$ T cells in the clodronate liposome-treated, but not in the selumetinib-treated groups (Fig. 5E–G). Notably, preferable effects were obtained from combination therapy (Fig. 5B–G). Taken together, our findings indicated that MEK inhibition combined with macrophage depletion could significantly suppress TNBC tumor growth and increase T lymphocyte infiltration.

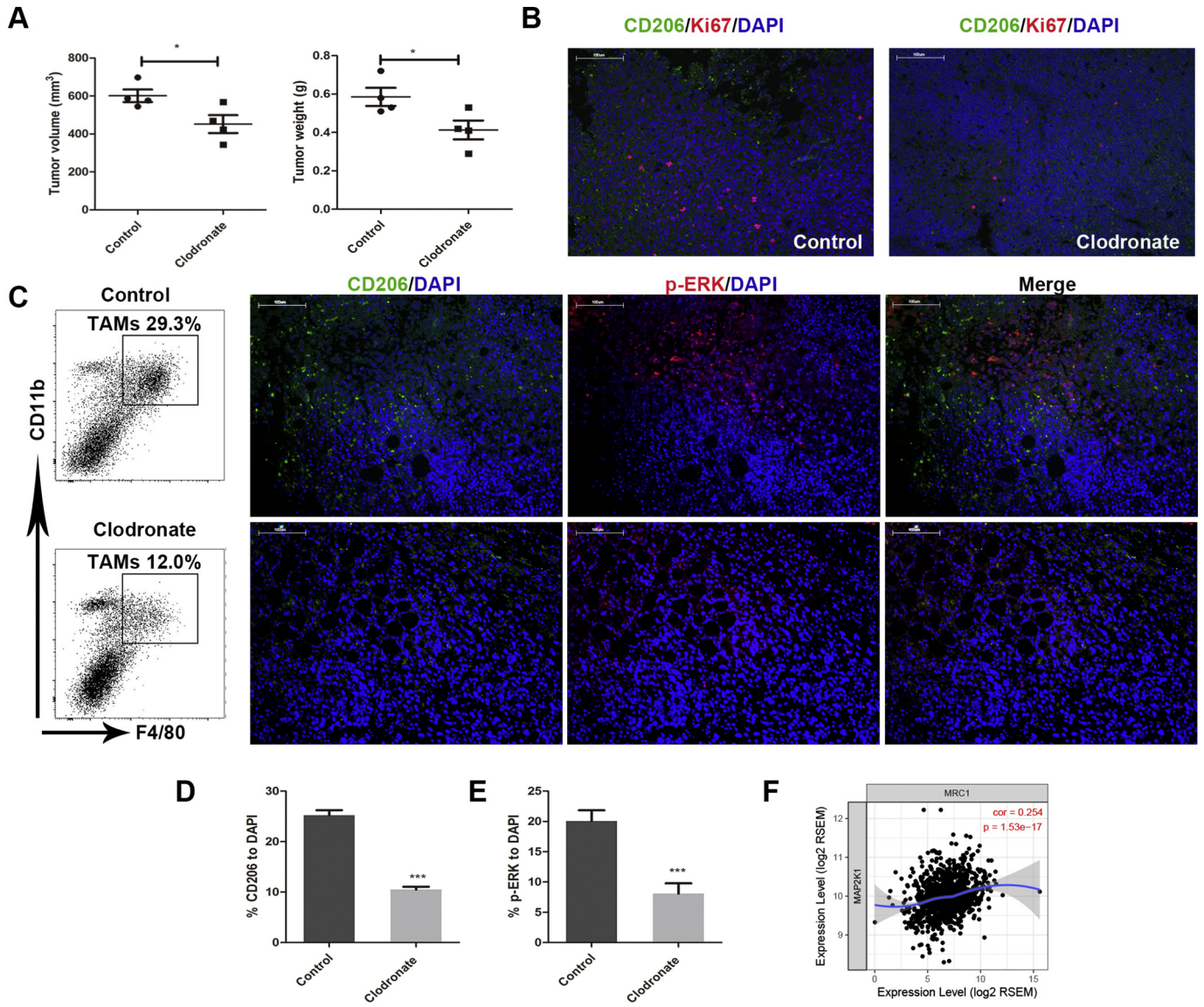

Fig. 3. Tumor-associated macrophage (TAM) depletion inhibits triple-negative breast cancer (TNBC) tumor growth and MAPK pathway activation.
(A) Tumor volumes (mm^3) and tumor weights (g) in individual groups of mice ($n = 4$). (B) Immunofluorescence staining of CD206 (green) and Ki-67 (red) in the tumor tissues from the control group (left) and from the clodronate liposome-treated group (right). Original magnification, ×200; scale bars = 100 μm. (C) Representative flow cytometric analyses of cancer infiltrating macrophages in tumors before TAM depletion (upper) and after TAM depletion (lower). Co-staining of CD206 (green) and p-ERK (red) in the tumor tissue sections from the control group (upper) and from the clodronate liposome-treated group (lower). Representative images are shown; original magnification, ×200; scale bars = 100 μm. The average relative number of CD206 (D) and p-ERK (E) fluorescent signals in cells were quantified in the tumor tissue sections from the control group and the clodronate liposome-treated group ($n = 4$). (F) *MRC-1* (CD206) and *MAP2K1* (ERK) mRNA expression based on the TCGA breast cancer dataset was analyzed by the online database Tumor IMmune Estimation Resource. Data are representative images or expressed as the mean ± SEM of each group from three separate experiments, $^*p < 0.05$, $^{**}p < 0.01$, $^{***}p < 0.001$. (For interpretation of the references to colour in this figure legend, the reader is referred to the web version of this article.)

4. Discussion

Here, we showed that TAMs might contribute to TNBC growth through MAPK pathway activation. Further, combined MEK inhibition and TAM depletion significantly restrained tumor growth in a TNBC mouse model. Macrophages comprise a diverse collection of cell types with different functional roles shaped by their tissue microenvironment. Traditionally, TAMs have been considered to have an anti-tumorigenic 'M1-like' phenotype and a pro-tumorigenic 'M2-like' phenotype [24]. In addition, TNBC cells have the strongest ability to activate macrophages to induce an M2-like phenotype, which in turn promotes tumor growth [11,12,25,26]. We and others have demonstrated that TAMs in TNBC models primarily comprise a subpopulation with an M2 phenotype, expressing high levels of CD206 [27]. An increased in ($CD206^+$) TAMs accompanied by proliferating tumor cells ($Ki67^+$) was observed by immunofluorescence in our study, indicating that TAMs might contribute to the highly proliferative feature of TNBC.

To further explore how TAMs support TNBC cell proliferation in the tumor microenvironment, we performed whole transcriptome analysis of 4 T1 cells incubated with TAMs and found that MAPK activation was significantly enhanced. This was consistent with our findings that M2 macrophage-conditioned medium alone was sufficient to increase p-ERK1/2 levels in TNBC cells. Thus, our results suggested that soluble mediators are generated to exert a pro-proliferative effect on TNBC cells. In the tumor microenvironment, growth factors function in an autocrine/paracrine manner to stimulate cancer progression [28]. Previous studies have shown that macrophage-derived EGF can regulate murine breast cancer cell stemness and promote tumor cell

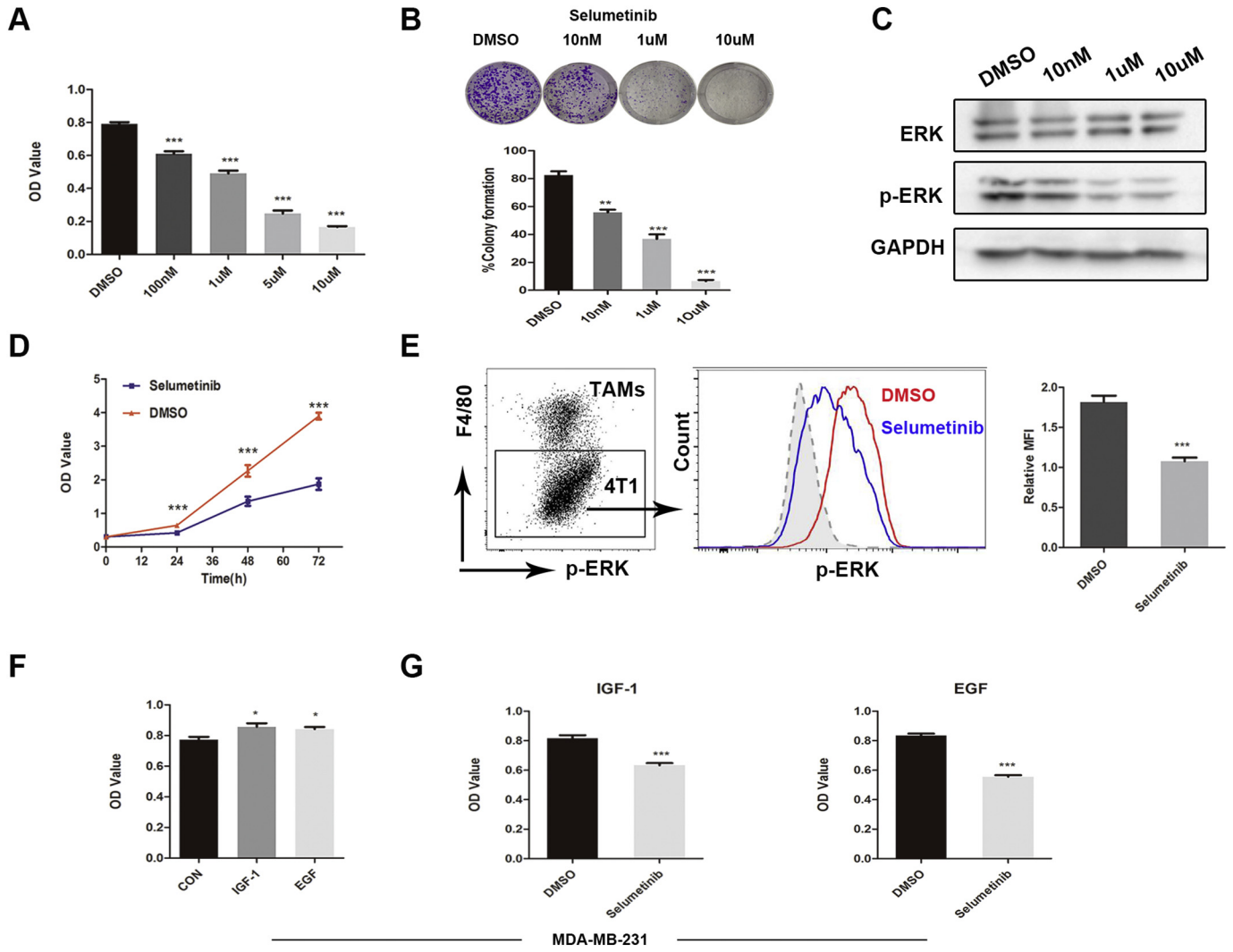

Fig. 4. Selumetinib inhibits 4 T1 cell proliferation and MAPK signaling in vitro.
(A) 4 T1 cells were treated with DMSO or 100 nM, 1 μM, 5 μM, or 10 μM of selumetinib for 48 h. Cell proliferation was assessed by CCK-8 assays ($n = 5$). (B) 4 T1 (10^3) cells were seeded into six-well plates and treated with DMSO or 10 nM, 1 μM, or 10 μM of selumetinib for 10 days. Colonies were then photographed under a camera. Colony numbers from seeded cells were presented as % colony formation as below ($n = 3$). (C) Western blotting analysis of ERK1/2 and phosphorylated ERK1/2 levels in 4 T1 cells treated with DMSO or indicated doses of selumetinib for 24 h. (D) 4 T1 cells (1×10^3) were cultured with 5×10^2 M2 macrophages in 96-well plates and treated with 1 μM selumetinib (blue) or DMSO (red) for 72 h, and cell proliferation was assessed by CCK-8 tests. (E) 4 T1 cells were co-cultured with M2 macrophages and then treated with 1 μM selumetinib (blue) or DMSO (red) for 24 h; phosphorylated ERK1/2 levels in 4 T1 cells were analyzed by flow cytometric analyses and isotype-stained cells are shown in grey. Relative mean fluorescence intensity (MFI) of ERK1/2 phosphorylation in 4 T1 cells is shown in each group at right (n = 4). (F) MDA-MB-231 cells were treated with normal culture medium, EGF (20 ng/mL), or IGF-1 (50 ng/mL) for 24 h. Cell proliferation was assessed by CCK-8 assays (n = 4). (G) MDA-MB-231 cells were treated with EGF (20 ng/mL) or IGF-1 (50 ng/mL), and each group was treated with 1 μM selumetinib or DMSO for 24 h. Cell proliferation was assessed by CCK-8 assays (n = 4). Data are representative images or expressed as the mean ± SEM of each group from three separate experiments, *$p < 0.05$, **$p < 0.01$, ***$p < 0.001$. (For interpretation of the references to colour in this figure legend, the reader is referred to the web version of this article.)

migration [10,22]. TAMs are the main sources of IGF-1in invasive breast cancer, and the blockade of insulin-like growth factors increases paclitaxel efficacy [7]. Moreover, autocrine HB-EGF promotes breast cancer metastasis and treatment with an HB-EGF inhibitor significantly reduces tumor growth [29,30]. TNBC cells express higher levels of TGF-α than non-TNBC cell lines and the TGFα–EGFR axis leads to cancer progression in TNBC patients [31]. In the current study, we assessed the growth factors involved in MAPK signaling and found that TNBC-treated macrophages express high levels of EGF, PDGFB, and IGF-1. Meanwhile, TAMs significantly induced the expression of HB-EGF, TGF-α, and TGFB3 in 4 T1 cells. Our results suggested that the enhanced autocrine/paracrine effects of growth factors might be involved in the pro-proliferative effect of TAMs on TNBC cells; these findings highlight the importance of TAMs in the tumor microenvironment.

In the current study, we demonstrated that TAM depletion in TNBC tumors decreases $CD206^+$ TAMs, promotes $CD4^+$ and $CD8\ T^+$ cell infiltration, and slows tumor growth. In contrast, selumetinib significantly suppressed tumor growth by blocking MAPK signaling. Most importantly, we found that preferable effects were obtained by concurrently blocking MAPK signaling and depleting TAMs. It is well established that TAMs comprise one of the central suppressive populations within tumors [24]. These cells suppress T cell functions through various mechanisms such as inhibiting naive T cell proliferation, producing immune checkpoint ligands, and secreting inhibitory cytokines [32–34]. Emerging evidence indicates that targeting TAMs could significantly promote T cell infiltration, which was found to be associated with improved survival in TNBC [35–37]. However, single-agent treatments to induce TAM depletion showed limited therapeutic effects

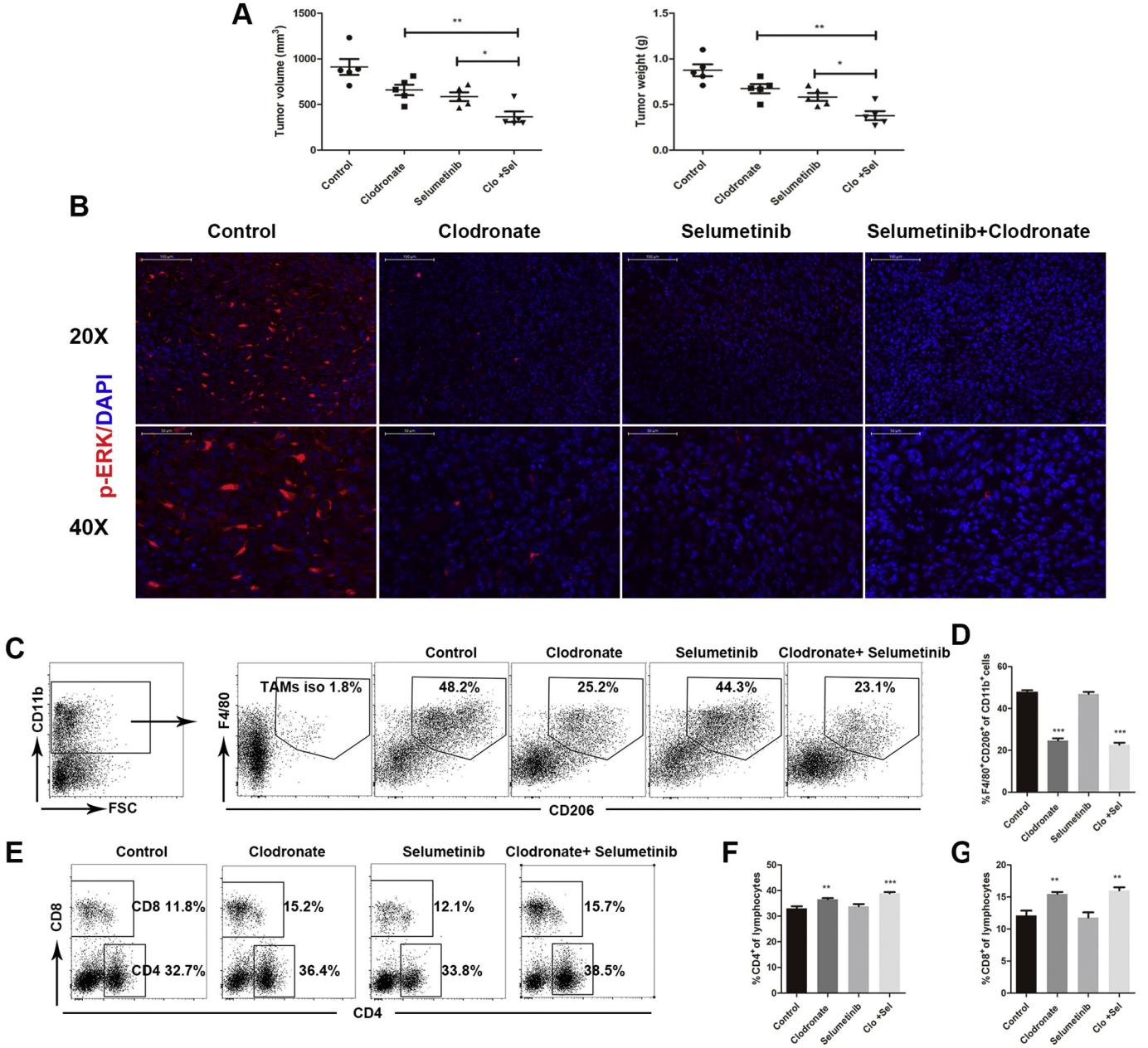

Fig. 5. Combining selumetinib with clodronate liposomes suppresses triple-negative breast cancer (TNBC) tumor growth and increases T lymphocyte infiltration. (A) Tumor volumes (mm^3) and tumor weights (g) in individual groups of mice (n = 5). (B) Immunofluorescence staining of p-ERK (red) in the tumor tissues sections from different groups. Scale bars = 100 μm (upper) and 50 μm (lower). (C) Representative flow cytometric analyses of tumor-associated macrophages (TAMs) in different groups. $CD11b^+$ cells were gated among cells from dissociated 4 T1 tumors, and $F4/80^+$ $CD206^+$ cells were then analyzed among $CD11b^+$ cells. (D) The percentages of $CD11b^+$ $F4/80^+$ $CD206^+$ TAMs among $CD11b^+$ cells from individual groups of mice were calculated (n = 4 per group). (E) Representative flow cytometric analyses of $CD4^+$ and $CD8^+$ T cells in different groups. Monocytes were first gated from total cells of dissociated 4 T1 tumors according to their SSC and FSC. $CD4^+$ and $CD8^+$ cells were gated in lymphocytes and the percentages of $CD4^+$ T cells (F) and $CD8^+$ T cells (G) from individual groups of mice are depicted (n = 4 per group). Data are representative images or expressed as the mean ± SEM of each group from three separate experiments, *p < 0.05, **p < 0.01, ***p < 0.001. (For interpretation of the references to colour in this figure legend, the reader is referred to the web version of this article.)

[23]. Therefore, the focus has changed to find combinations with other agents. Previous studies have shown that targeting tumor-infiltrating macrophages improves chemotherapeutic responses in preclinical models of pancreatic and breast cancer [38,39]. Combining TAM depletion with checkpoint immunotherapy was found to induce tumor regression in a pancreatic cancer model [36]. Synergism with TAM depletion could also improve the radiotherapy efficacy in a prostate cancer model [35]. Together, these findings indicate that preferable responses might be obtained by combining macrophage depletion with other anti-cancer therapies [40]. Meanwhile, our results showed that TAMs enhance MAPK signaling in TNBC. Consistently, a recent study reported that stromal cells contribute to the proliferative phenotype of pancreatic cancer through MAPK signaling [15]. MAPK pathway activation was also found to be one of the most important intrinsic properties of TNBC in both genetically-engineered mouse models and in human patients [16]. Accumulative evidence indicates that blocking MAPK signaling with MEK inhibitors is a promising approach to suppress TNBC progression [41–43]. Therefore, our data suggest that combination of MEK inhibitors and TAM depletion could be an alternative option to treat TNBC.

However, there are limitations to our study. First, the combination of MEK inhibitors and TAM depletion is encouraging based on the short-term efficacy; however, we will need to perform long-term observations to check whether drug resistance occurs. In addition, there are also biological restrictions associated with using a mouse cell line as a cancer model, and thus, we will investigate patient-derived tumor samples to further support our data.

In conclusion, our observations revealed that TAMs contribute to TNBC tumor growth through MAPK pathway activation, which is positively correlated with TAM infiltration. Combining selumetinib with clodronate liposomes could suppress MAPK signaling, promote $CD4^+$ and $CD8\ T^+$ cell infiltration, and restrain tumor growth in a TNBC mouse model. Our findings might thus suggest new therapeutic options for TNBC intervention.

Supplementary data to this article can be found online at https://doi.org/10.1016/j.intimp.2019.105864.

Declaration of competing interest

All authors declared no competing interests.

Acknowledgments

We thank Guo Di and Shen Xi (Huazhong University of Science and Technology) for assistance with flow cytometry and Western blotting.

Funding information

This work was supported by laboratory of general surgery department, Union Hospital, Tongji Medical College, Huazhong University of Science and Technology.

Data availability

The TCGA datasets analyzed during the study are publically available at [20,21]. The data discussed in this publication have been deposited in NCBI's Gene Expression Omnibus (Edgar et al., 2002) and are accessible through GEO series accession number GSE134787 (https://www.ncbi.nlm.nih.gov/geo/query/acc.cgi?acc=GSE134787).

References

[1] W. Chen, R. Zheng, P.D. Baade, S. Zhang, H. Zeng, F. Bray, A. Jemal, X.Q. Yu, J. He, Cancer statistics in China, 2015, CA Cancer J. Clin. 66 (2) (2016) 115–132.
[2] C. Neophytou, P. Boutsikos, P. Papageorgis, Molecular mechanisms and emerging therapeutic targets of triple-negative breast cancer metastasis, Front. Oncol. 8 (2018) 31.
[3] C. Liedtke, C. Mazouni, K.R. Hess, F. Andre, A. Tordai, J.A. Mejia, W.F. Symmans, A.M. Gonzalez-Angulo, B. Hennessy, M. Green, et al., Response to neoadjuvant therapy and long-term survival in patients with triple-negative breast cancer, Am. J. Clin. Oncol. 26 (8) (2008) 1275–1281.
[4] J.W. Pollard, Macrophages define the invasive microenvironment in breast cancer, J. Leukoc. Biol. 84 (3) (2008) 623–630.
[5] M. Viitala, R. Virtakoivu, S. Tadayon, J. Rannikko, S. Jalkanen, M. Hollmen, Immunotherapeutic blockade of macrophage clever-1 reactivates the CD8(+) T-cell response against immunosuppressive tumors, Clin. Cancer Res. 25 (11) (2019) 3289–3303.
[6] Y. Miyasato, T. Shiota, K. Ohnishi, C. Pan, H. Yano, H. Horlad, Y. Yamamoto, M. Yamamoto-Ibusuki, H. Iwase, M. Takeya, et al., High density of CD204-positive macrophages predicts worse clinical prognosis in patients with breast cancer, Cancer Sci. 108 (8) (2017) 1693–1700.
[7] L. Ireland, A. Santos, F. Campbell, C. Figueiredo, D. Hammond, L.G. Ellies, U. Weyer-Czernilofsky, T. Bogenrieder, M. Schmid, A. Mielgo, Blockade of insulin-like growth factors increases efficacy of paclitaxel in metastatic breast cancer, Oncogene 37 (15) (2018) 2022–2036.
[8] M.J. Campbell, N.Y. Tonlaar, E.R. Garwood, D. Huo, D.H. Moore, A.I. Khramtsov, A. Au, F. Baehner, Y. Chen, D.O. Malaka, et al., Proliferating macrophages associated with high grade, hormone receptor negative breast cancer and poor clinical outcome, Breast Cancer Res. Treat. 128 (3) (2011) 703–711.
[9] S. Aharinejad, P. Paulus, M. Sioud, M. Hofmann, K. Zins, R. Schafer, E.R. Stanley, D. Abraham, Colony-stimulating factor-1 blockade by antisense oligonucleotides and small interfering RNAs suppresses growth of human mammary tumor xenografts in mice, Cancer Res. 64 (15) (2004) 5378–5384.
[10] J. Yang, D. Liao, C. Chen, Y. Liu, T.H. Chuang, R. Xiang, D. Markowitz, R.A. Reisfeld, Y. Luo, Tumor-associated macrophages regulate murine breast cancer stem cells through a novel paracrine EGFR/Stat3/Sox-2 signaling pathway, Stem Cells 31 (2) (2013) 248–258.
[11] S. Su, Q. Liu, J. Chen, J. Chen, F. Chen, C. He, D. Huang, W. Wu, L. Lin, W. Huang, et al., A positive feedback loop between mesenchymal-like cancer cells and macrophages is essential to breast cancer metastasis, Cancer Cell 25 (5) (2014) 605–620.
[12] D.A. Stewart, Y. Yang, L. Makowski, M.A. Troester, Basal-like breast cancer cells induce phenotypic and genomic changes in macrophages, Mol. Cancer Res. 10 (6) (2012) 727–738.
[13] J.A. McCubrey, L.S. Steelman, W.H. Chappell, S.L. Abrams, E.W. Wong, F. Chang, B. Lehmann, D.M. Terrian, M. Milella, A. Tafuri, et al., Roles of the Raf/MEK/ERK pathway in cell growth, malignant transformation and drug resistance, Biochim. Biophys. Acta 1773 (8) (2007) 1263–1284.
[14] L. Santarpia, S.M. Lippman, A.K. El-Naggar, Targeting the MAPK-RAS-RAF signaling pathway in cancer therapy, Expert Opin. Ther. Targets 16 (1) (2012) 103–119.
[15] M. Ligorio, S. Sil, J. Malagon-Lopez, L.T. Nieman, S. Misale, M. Di Pilato, R.Y. Ebright, M.N. Karabacak, A.S. Kulkarni, A. Liu, et al., Stromal microenvironment shapes the intratumoral architecture of pancreatic cancer, Cell 178 (1) (2019) 160–175.
[16] H. Liu, C.J. Murphy, F.A. Karreth, K.B. Emdal, F.M. White, O. Elemento, A. Toker, G.M. Wulf, L.C. Cantley, Identifying and targeting sporadic oncogenic genetic aberrations in mouse models of triple-negative breast cancer, Cancer Discov. 8 (3) (2018) 354–369.
[17] X. Shen, J. Zhong, P. Yu, Q. Zhao, T. Huang, YY1-regulated LINC00152 promotes triple negative breast cancer progression by affecting on stability of PTEN protein, Biochem. Biophys. Res. Commun. 509 (2) (2019) 448–454.
[18] D.G. DeNardo, J.B. Barreto, P. Andreu, L. Vasquez, D. Tawfik, N. Kolhatkar, L.M. Coussens, CD4(+) T cells regulate pulmonary metastasis of mammary carcinomas by enhancing protumor properties of macrophages, Cancer Cell 16 (2) (2009) 91–102.
[19] H. Lu, K.R. Clauser, W.L. Tam, J. Frose, X. Ye, E.N. Eaton, F. Reinhardt, V.S. Donnenberg, R. Bhargava, S.A. Carr, et al., A breast cancer stem cell niche supported by juxtacrine signalling from monocytes and macrophages, Nat. Cell Biol. 16 (11) (2014) 1105–1117.
[20] Z. Tang, C. Li, B. Kang, G. Gao, C. Li, Z. Zhang, GEPIA: a web server for cancer and normal gene expression profiling and interactive analyses, Nucleic Acids Res. 45 (W1) (2017) W98–W102.
[21] T. Li, J. Fan, B. Wang, N. Traugh, Q. Chen, J.S. Liu, B. Li, X.S. Liu, TIMER: a web server for comprehensive analysis of tumor-infiltrating immune cells, Cancer Res. 77 (21) (2017) e108–e110.
[22] S. Goswami, E. Sahai, J.B. Wyckoff, M. Cammer, D. Cox, F.J. Pixley, E.R. Stanley, J.E. Segall, J.S. Condeelis, Macrophages promote the invasion of breast carcinoma cells via a colony-stimulating factor-1/epidermal growth factor paracrine loop, Cancer Res. 65 (12) (2005) 5278–5283.
[23] V. Kumar, L. Donthireddy, D. Marvel, T. Condamine, F. Wang, S. Lavilla-Alonso, A. Hashimoto, P. Vonteddu, R. Behera, M.A. Goins, et al., Cancer-associated fibroblasts neutralize the anti-tumor effect of CSF1 receptor blockade by inducing PMN-MDSC infiltration of tumors, Cancer Cell 32 (5) (2017) 654–668 e655.
[24] D.G. DeNardo, B. Ruffell, Macrophages as regulators of tumour immunity and immunotherapy, Nat. Rev. Immunol. 19 (6) (2019) 369–382.
[25] Z.Y. Yuan, R.Z. Luo, R.J. Peng, S.S. Wang, C. Xue, High infiltration of tumor-associated macrophages in triple-negative breast cancer is associated with a higher risk of distant metastasis, OncoTargets and therapy 7 (2014) 1475–1480.
[26] H.J. Cho, J.I. Jung, D.Y. Lim, G.T. Kwon, S. Her, J.H. Park, J.H. Park, Bone marrow-derived, alternatively activated macrophages enhance solid tumor growth and lung metastasis of mammary carcinoma cells in a Balb/C mouse orthotopic model, Breast Cancer Res. 14 (3) (2012) R81.
[27] A. Mantovani, S. Sozzani, M. Locati, P. Allavena, A. Sica, Macrophage polarization: tumor-associated macrophages as a paradigm for polarized M2 mononuclear phagocytes, Trends Immunol. 23 (11) (2002) 549–555.
[28] C. Neuzillet, A. Tijeras-Raballand, L. de Mestier, J. Cros, S. Faivre, E. Raymond, MEK in cancer and cancer therapy, Pharmacol. Ther. 141 (2) (2014) 160–171.
[29] F. Yotsumoto, E. Oki, E. Tokunaga, Y. Maehara, M. Kuroki, S. Miyamoto, HB-EGF orchestrates the complex signals involved in triple-negative and trastuzumab-resistant breast cancer, Int. J. Cancer 127 (11) (2010) 2707–2717.
[30] Z.N. Zhou, V.P. Sharma, B.T. Beaty, M. Roh-Johnson, E.A. Peterson, N. Van Rooijen, P.A. Kenny, H.S. Wiley, J.S. Condeelis, J.E. Segall, Autocrine HBEGF expression promotes breast cancer intravasation, metastasis and macrophage-independent invasion in vivo, Oncogene 33 (29) (2014) 3784–3793.
[31] R.M.C. Ignacio, C.R. Gibbs, E.S. Lee, D.S. Son, The TGFalpha-EGFR-Akt signaling axis plays a role in enhancing proinflammatory chemokines in triple-negative breast cancer cells, Oncotarget 9 (50) (2018) 29286–29303.
[32] A.L. Doedens, C. Stockmann, M.P. Rubinstein, D. Liao, N. Zhang, D.G. DeNardo, L.M. Coussens, M. Karin, A.W. Goldrath, R.S. Johnson, Macrophage expression of hypoxia-inducible factor-1 alpha suppresses T-cell function and promotes tumor progression, Cancer Res. 70 (19) (2010) 7465–7475.
[33] D.M. Kuang, Q. Zhao, C. Peng, J. Xu, J.P. Zhang, C. Wu, L. Zheng, Activated monocytes in peritumoral stroma of hepatocellular carcinoma foster immune privilege and disease progression through PD-L1, J. Exp. Med. 206 (6) (2009) 1327–1337.
[34] B. Ruffell, D. Chang-Strachan, V. Chan, A. Rosenbusch, C.M. Ho, N. Pryer, D. Daniel, E.S. Hwang, H.S. Rugo, L.M. Coussens, Macrophage IL-10 blocks CD8+ T cell-dependent responses to chemotherapy by suppressing IL-12 expression in

intratumoral dendritic cells, Cancer Cell 26 (5) (2014) 623–637.
[35] J. Xu, J. Escamilla, S. Mok, J. David, S. Priceman, B. West, G. Bollag, W. McBride, L. Wu, CSF1R signaling blockade stanches tumor-infiltrating myeloid cells and improves the efficacy of radiotherapy in prostate cancer, Cancer Res. 73 (9) (2013) 2782–2794.
[36] Y. Zhu, B.L. Knolhoff, M.A. Meyer, T.M. Nywening, B.L. West, J. Luo, A. Wang-Gillam, S.P. Goedegebuure, D.C. Linehan, D.G. DeNardo, CSF1/CSF1R blockade reprograms tumor-infiltrating macrophages and improves response to T-cell checkpoint immunotherapy in pancreatic cancer models, Cancer Res. 74 (18) (2014) 5057–5069.
[37] S. Loi, S. Michiels, R. Salgado, N. Sirtaine, V. Jose, D. Fumagalli, P.L. Kellokumpu-Lehtinen, P. Bono, V. Kataja, C. Desmedt, et al., Tumor infiltrating lymphocytes are prognostic in triple negative breast cancer and predictive for trastuzumab benefit in early breast cancer: results from the FinHER trial, Ann. Oncol. 25 (8) (2014) 1544–1550.
[38] J.B. Mitchem, D.J. Brennan, B.L. Knolhoff, B.A. Belt, Y. Zhu, D.E. Sanford, L. Belaygorod, D. Carpenter, L. Collins, D. Piwnica-Worms, et al., Targeting tumor-infiltrating macrophages decreases tumor-initiating cells, relieves immunosuppression, and improves chemotherapeutic responses, Cancer Res. 73 (3) (2013) 1128–1141.
[39] D.G. DeNardo, D.J. Brennan, E. Rexhepaj, B. Ruffell, S.L. Shiao, S.F. Madden, W.M. Gallagher, N. Wadhwani, S.D. Keil, S.A. Junaid, et al., Leukocyte complexity predicts breast cancer survival and functionally regulates response to chemotherapy, Cancer Discov. 1 (1) (2011) 54–67.
[40] B. Ruffell, L.M. Coussens, Macrophages and therapeutic resistance in cancer, Cancer Cell 27 (4) (2015) 462–472.
[41] C. Bartholomeusz, X. Xie, M.K. Pitner, K. Kondo, A. Dadbin, J. Lee, H. Saso, P.D. Smith, K.N. Dalby, N.T. Ueno, MEK inhibitor selumetinib (AZD6244; ARRY-142886) prevents lung metastasis in a triple-negative breast cancer xenograft model, Mol. Cancer Ther. 14 (12) (2015) 2773–2781.
[42] J. Lee, B. Lim, T. Pearson, K. Choi, J.A. Fuson, C. Bartholomeusz, L.J. Paradiso, T. Myers, D. Tripathy, N.T. Ueno, Anti-tumor and anti-metastasis efficacy of E6201, a MEK1 inhibitor, in preclinical models of triple-negative breast cancer, Breast Cancer Res. Treat. 175 (2) (2019) 339–351.
[43] J. Lee, R. Galloway, G. Grandjean, J. Jacob, J. Humphries, C. Bartholomeusz, S. Goodstal, B. Lim, G. Bartholomeusz, N.T. Ueno, et al., Comprehensive two- and three-dimensional RNAi screening identifies PI3K inhibition as a complement to MEK inhibitor AS703026 for combination treatment of triple-negative breast cancer, J. Cancer 6 (12) (2015) 1306–1319.